



Reactor staging influences microbial community composition and diversity of denitrifying MBBRs- Implications on pharmaceutical removal

Torresi, Elena; Gülay, Arda; Polesel, Fabio; Jensen, Marlene Mark; Christensson, Magnus; Smets, Barth F.; Plósz, Benedek G.

Published in:
Water Research

Link to article, DOI:
[10.1016/j.watres.2018.03.014](https://doi.org/10.1016/j.watres.2018.03.014)

Publication date:
2018

Document Version
Peer reviewed version

[Link back to DTU Orbit](#)

Citation (APA):
Torresi, E., Gülay, A., Polesel, F., Jensen, M. M., Christensson, M., Smets, B. F., & Plósz, B. G. (2018). Reactor staging influences microbial community composition and diversity of denitrifying MBBRs- Implications on pharmaceutical removal. *Water Research*, 138, 333-345. <https://doi.org/10.1016/j.watres.2018.03.014>

General rights

Copyright and moral rights for the publications made accessible in the public portal are retained by the authors and/or other copyright owners and it is a condition of accessing publications that users recognise and abide by the legal requirements associated with these rights.

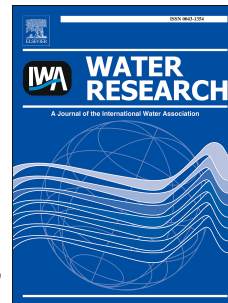
- Users may download and print one copy of any publication from the public portal for the purpose of private study or research.
- You may not further distribute the material or use it for any profit-making activity or commercial gain
- You may freely distribute the URL identifying the publication in the public portal

If you believe that this document breaches copyright please contact us providing details, and we will remove access to the work immediately and investigate your claim.

Accepted Manuscript

Reactor staging influences microbial community composition and diversity of denitrifying MBBRs- Implications on pharmaceutical removal

Elena Torresi, Arda Gülay, Fabio Polese, Marlene M. Jensen, Magnus Christensson, Barth F. Smets, Benedek Gy. Plósz



PII: S0043-1354(18)30194-5

DOI: [10.1016/j.watres.2018.03.014](https://doi.org/10.1016/j.watres.2018.03.014)

Reference: WR 13633

To appear in: *Water Research*

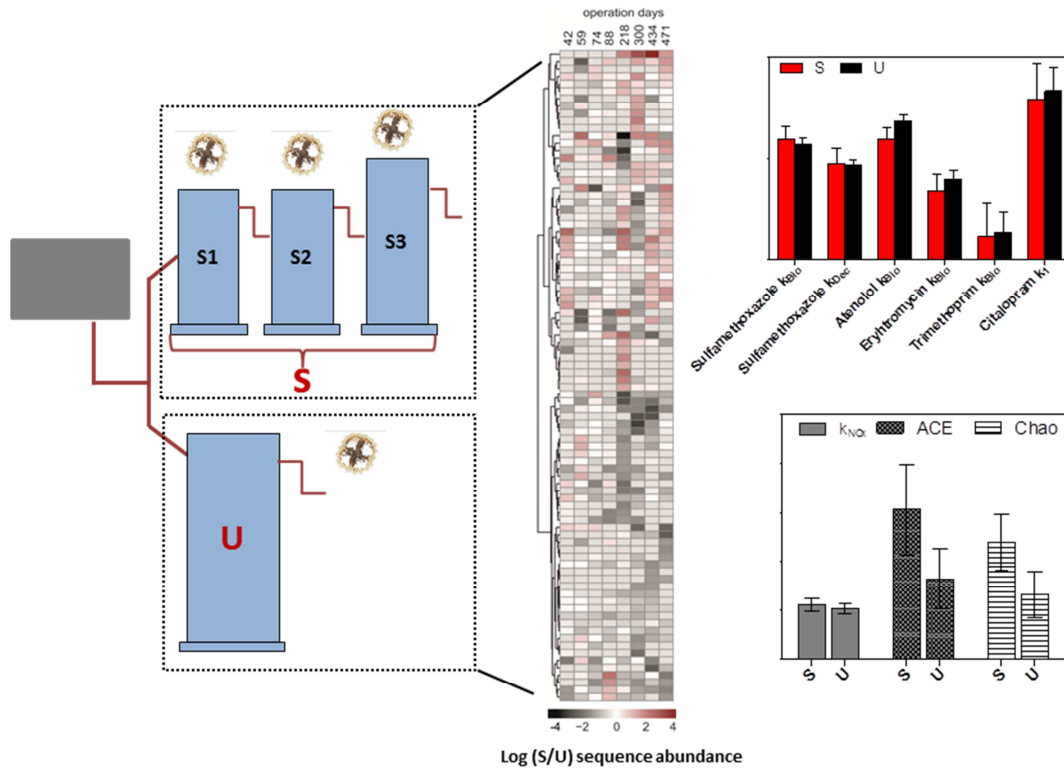
Received Date: 9 November 2017

Revised Date: 16 February 2018

Accepted Date: 6 March 2018

Please cite this article as: Torresi, E., Gülay, A., Polese, F., Jensen, M.M., Christensson, M., Smets, B.F., Plósz, B.G., Reactor staging influences microbial community composition and diversity of denitrifying MBBRs- Implications on pharmaceutical removal, *Water Research* (2018), doi: 10.1016/j.watres.2018.03.014.

This is a PDF file of an unedited manuscript that has been accepted for publication. As a service to our customers we are providing this early version of the manuscript. The manuscript will undergo copyediting, typesetting, and review of the resulting proof before it is published in its final form. Please note that during the production process errors may be discovered which could affect the content, and all legal disclaimers that apply to the journal pertain.



1 Reactor staging influences microbial community
2 composition and diversity of denitrifying MBBRs-
3 Implications on pharmaceutical removal

4 Elena Torresi^{1,2,**}, Arda Gülay¹, Fabio Polesel¹, Marlene M. Jensen¹, Magnus
5 Christensson², Barth F. Smets^{1*}, Benedek Gy. Plósz^{1,3}

6
7 ¹DTU Environment, Technical University of Denmark, Bygningstorvet B115, 2800 Kongens Lyngby,
8 Denmark

9 ²Veolia Water Technologies AB, AnoxKaldnes, Klosterängsvägen 11A, SE-226 47 Lund, Sweden

10 ³Department of Chemical Engineering, University of Bath, Claverton Down, Bath BA2 7AY, UK

11 *Corresponding authors: elto@env.dtu.dk, bfsm@env.dtu.dk

12

13 Abstract

14 The subdivision of biofilm reactor in two or more stages (i.e., reactor staging) represents an option for
15 process optimisation of biological treatment. In our previous work, we showed that the gradient of
16 influent organic substrate availability (induced by the staging) can influence the microbial activity (i.e.,
17 denitrification and pharmaceutical biotransformation kinetics) of a denitrifying three-stage Moving Bed
18 Biofilm Reactor (MBBR) system. However, it is unclear whether staging and thus the long-term
19 exposure to varying organic carbon type and loading influences the microbial community structure and
20 diversity. In this study, we investigated biofilm structure and diversity in the three-stage MBBR system
21 (S) compared to a single-stage configuration (U) and their relationship with microbial functions.
22 Results from 16S rRNA amplicon libraries revealed a significantly higher microbial richness in the
23 staged MBBR (at 99% sequence similarity) compared to single-stage MBBR. A more even and diverse
24 microbial community was selected in the last stage of S (S3), likely due to exposure to carbon
25 limitation during continuous-flow operation. A core of OTUs was shared in both systems, consisting of
26 *Burkholderiales*, *Xanthomonadales*, *Flavobacteriales* and *Sphingobacteriales*, while MBBR staging
27 selected for specific taxa (i.e., *Candidatus division WS6* and *Deinococcales*). Results from quantitative
28 PCR (qPCR) showed that S3 exhibited the lowest abundance of 16S rRNA but the highest abundance
29 of *atypical nosZ*, suggesting a selection of microbes with more diverse N-metabolism (i.e., not-
30 complete denitrifiers) in the stage exposed to the lowest carbon availability. A positive correlation
31 ($p < 0.05$) between removal rate constants of several pharmaceuticals with abundance of relevant
32 denitrifying genes was observed, but not with biodiversity. Despite the previously suggested positive
33 relationship between microbial diversity and functionality in macrobial and microbial ecosystems, this

34 was not observed in the current study, suggesting a need to further investigate structure-function
35 relationships for denitrifying systems.

36

37 **Keywords:** Moving Bed Biofilm Reactors, micropollutant removal, organic carbon, structure-function
38 relationships, heterotrophic denitrification

39

1. Introduction

The presence of micropollutants (e.g., pharmaceutical and personal care products) in municipal wastewater effluent is well documented (Barbosa et al., 2016) and has been associated to several environmental risks (Painter et al., 2009).

Existing processes in conventional wastewater treatment plants (WWTPs) do not represent an efficient barrier against the release of micropollutants with treated effluent streams (Carballa et al., 2004). Hence, a number of engineering solutions are being explored to optimize the removal of micropollutants via biological wastewater treatment (Falås et al., 2016; Torresi et al., 2017, 2016).

The subdivision of biological reactors in two or more stages (i.e. reactor staging) has recently been proposed to enhance the removal of conventional pollutants (i.e., organic carbon, nitrogen) and pharmaceuticals in biofilm systems such as Moving Bed Biofilm Reactors (MBBRs) (Escolà Casas et al., 2015; Polesel et al., 2017). In MBBRs, biofilms grow on specifically designed plastic carriers, which are suspended and retained in the system (Ødegaard, 1999).

Due to presence of different fractions of organic carbon (e.g., from readily and slowly biodegradable to recalcitrant) in wastewater (Roeleveld and Van Loosdrecht, 2002), biofilm retained in different MBBR stages can be likely exposed to different substrate type and availability conditions. Based on long and short-term laboratory experiments, our previous work (Polesel et al., 2017) showed that the first stage of a pre-denitrifying three-stage MBBR system (S1) was effectively exposed to higher loadings of easily degradable organic carbon compared to the last stage (S3). Consequently, the first and last stage of the staged MBBR system exhibited, respectively, the highest and lowest denitrification and micropollutant biotransformation rate constant during targeted batch experiments (Polesel et al., 2017). However, it remains unclear: (i) if these differences in denitrification and biotransformation kinetics

62 are related to the microbial community structure and diversity, induced by organic carbon availability;
63 and (ii) if this results in major differences in the overall performance of three-stage MBBR system
64 compared to a single-stage configuration.

65 Wastewater organic carbon availability has previously been shown to differently shape the structure
66 and diversity of microbial communities of denitrifying (Xia et al., 2010), aerobic MBBR (Fu et al.,
67 2010), and in aquifer sediment system (Li et al., 2012, 2013), an effect that was found to correlate with
68 micropollutants removal efficiency (Alidina et al., 2014). Hence, elucidating the microbial structure
69 and diversity in biofilm systems and its influence on the overall microbial activity is fundamental for
70 providing a basis to improve design and operation of MBBR systems towards pharmaceuticals
71 removal. Additionally, although denitrification is a widespread process in biological wastewater
72 treatment, substantial knowledge gaps remain concerning microbial communities under denitrifying
73 condition (Lu et al., 2014).

74 Investigating microbial composition and diversity (i.e., α -diversity) in biological systems appears
75 especially important when assessing rare microbial functions, such as biotransformation of
76 micropollutants (Helbling et al., 2015; Johnson et al., 2015a). The existence of a relationship between
77 microbial diversity and activity has been debated but a positive relationship between biodiversity and
78 ecosystem functionality is commonly accepted (Briones and Raskin, 2003). This relationship has been
79 observed with respect to the biotransformation of several micropollutants in both full-scale (Johnson et
80 al., 2015a) and laboratory- scale bioreactors (Torresi et al., 2016; Stadler et al., 2016), suggesting that
81 communities with higher diversity are likely to have more functional traits (Johnson et al., 2015b).
82 Accordingly, biofilms, potentially exhibiting more microbial niches and thus higher biodiversity than
83 conventional activated sludge (Stewart and Franklin, 2008), can represent a valid option to enhance
84 micropollutant removal. Furthermore, the exposure of biofilm to varying carbon types and conditions

85 through bioreactor staging could additionally positively impact biofilm microbial diversity– the core
86 hypothesis tested herein.

87 In this study we evaluated the long-term effects of three-stage (S=S1+S2+S3) and single-stage
88 configurations (U) of pre-denitrifying MBBR on the biofilm microbial community composition and
89 diversity. High-throughput sequencing of 16S rRNA gene amplicon and quantitative PCR (qPCR) were
90 used to assess microbial diversity at local (S1, S2, S3) and system (S, U) level and the abundance of
91 relevant denitrifying genes, respectively. Thus, the main objectives of the study were:

- 92 1) to investigate the effect of organic carbon availability tiered by staging MBBRs on microbial
93 composition and diversity at local and system level, benchmarked against a single-stage
94 configuration;
- 95 2) to assess the dynamics in microbial community composition and denitrifying genes abundance
96 in the two MBBR systems during long term operation;
- 97 3) to assess associations between micropollutant biotransformation, local/system diversity and
98 denitrifying functionalities.

99 2. Methods

100 2.1. Continuous-flow operation of the MBBRs and batch experiments.

101 A detailed description of the three- and single stage MBBR systems is given in Polesel et al. 2017.
102 Briefly, two laboratory scale pre-denitrifying MBBR system with K1 carriers (AnoxKaldnes, Lund,
103 Sweden) were operated in parallel under continuous-flow conditions for 1.5 years.

104 The single-stage system included a single bioreactor (U) with an operating volume of 6 L. The three-
105 stage configuration included three reactors in series (S1, S2, S3) with a total operating volume of 6 L
106 (1.5 L for S1 and S2 and 3 L for S3). The two systems were operated under identical conditions, i.e.
107 influent flow rate, hydraulic residence time (HRT= 8.9 h), filling ratio (33%), ambient temperature,
108 medium characteristics (pre-clarified wastewater from Mølleåværket WWTP, Lundtofte, Denmark),
109 influent nitrate concentration ($\sim 103 \text{ mgN L}^{-1}$), sparging of N_2 gas for mixing and to ensure anoxic
110 conditions (see Table S1 in Supplementary Information). The systems were started with MBBR
111 carriers collected from the post-denitrification zone of Sjölanda WWTP (Malmö, Sweden), operated
112 with external methanol dosing, as carbon source.

113 Two batch experiments were performed with the aim to assess denitrification rates and
114 biotransformation rate constants of micropollutants at day 100 (Batch 1, after reaching a stable COD
115 and nitrogen removal of ca. 70% and 44%, respectively) and day 471 (Batch 2, at the end of the
116 experiment) (Polesel et al., 2017). For the batch experiments, the flow to and between reactors was
117 stopped and the reactors were drained. Subsequently, the reactors were filled with pre-clarified
118 wastewater (grab sampled with an initial $\text{NO}_3\text{-N}$ concentration of $100\text{-}104 \text{ mgNL}^{-1}$) and carriers from
119 U, S1, S2 and S3 (20% and 10% of filling ratio for Batch 1 and 2, respectively). The experiment lasted
120 for 24 and 49 h for Batch 1 and 2, respectively, and 10 samples of aqueous solution were withdrawn

121 for micropollutants analysis at regular intervals (0, 0.3, 0.7, 1.2, 1.7, 2.2, 4.3, 7.5, and 10.3, 20 h for
122 Batch 1 and additionally at 49 h for Batch 2). A fixed number of carriers was removed to maintain a
123 constant filling ratio during batch experiments. The experiments were performed at ambient
124 temperature (i.e., 20.3 ± 0.05 °C in Batch 1 and 16.9 ± 0.4 °C in Batch 2) and pH was adjusted to $8 \pm$
125 0.5 with 1M HCl spikes. Further details on the batch experiment can be found in Polesel et al. (2017).

126

127 **2.2 DNA extraction and quantitative PCR.**

128 To characterize microbial composition and its variation over long-term operation of the two MBBR
129 systems, biofilm carriers for each MBBR were collected at day 0 (inoculum sample), 42, 59, 74, 88,
130 218, 300, 434 and 471 of operation. Samples were collected with the highest frequency during the first
131 100 days of operation to assess biomass adaption to the new operational conditions (i.e., staged pre-
132 denitrification without methanol addition). A prior analysis of biological replicates (2 different carriers)
133 at day 0 showed that the biomass from one carrier provided a sufficient descriptor of the entire
134 community (results are discussed in section S1 of supplementary information and in Fig. S1). Each
135 time, biomass was detached from one carrier using a sterile brush (Gynobrush, Dutscher Scientific) and
136 sterile-filtered tap water, centrifuged (10000 rpm for 5 minutes), and the supernatant was removed. The
137 sample was stored at -20 °C until further analysis. DNA was extracted from attached biomass of one
138 carrier using a Fast DNA spin kit for soils (MP Biomedicals, USA) following manufacturer's
139 instructions. The quantity and quality of DNA were measured and checked by its 260/280 ratio by
140 NanoDrop (Thermo Scientific™). Quantitative PCR (qPCR) was performed to estimate the abundance
141 of total bacteria (EUB) with non-specific 16S rRNA gene targeted primers, and the abundance of a
142 suite of genes encoding relevant functions: nitrate reductase (*narG*), cytochrome cd1 and copper nitrite
143 reductases (*nirK* and *nirS*, respectively) nitrous oxide reductase of the *Proteobacteria nosZ* variant

144 (*nosZ* typical) and of the *nosZ* variant (*nosZ* atypical). Reported total microbial abundances are
145 expressed as number of gene copies per gram of biomass. Primers and conditions for quantification of
146 each gene are listed in Table S2.

147

148 **2.3. 16S rRNA gene amplification, sequencing and bioinformatic analysis.**

149 DNA extracted as described in 2.2 was also used for 16S rRNA analysis by Illumina MiSeq. PCR
150 amplification and sequencing were performed at the DTU Multi Assay Core Center (Kgs Lyngby, DK).

151 Briefly, extracted DNA was PCR amplified using 16S rRNA bacterial gene primers PRK341F (5'-
152 CCTAYGGGRBGCASCAG-3') and PRK806R (5'-GGACTACNNGGGTATCTAAT-3')(Yu et al.,

153 2005) targeting the V3 and V4 region. PCR products were purified using AMPure XP beads
154 (Beckman-Coulter) prior to index PCR (Nextera XT, Illumina) and sequencing by Illumina MiSeq.

155 Paired-end reads were assembled and screenings were implemented using mothur (Schloss, 2009).

156 High quality sequences were then transferred to the QIIME environment and OTUs were picked at 93,

157 95, 97 and 99% sequence similarity using the UCLUST algorithm with default settings, and

158 representative sequences from each were aligned against the Silva123_SSURef reference alignment

159 using SINA algorithm. Aligned sequences were then used to build phylogenetic trees using the Fast

160 Tree method (Price et al., 2009).

161 Taxonomy assignment of each representative sequence at all similarity levels was implemented using

162 the BLAST algorithm against the Silva128_SSURef database. Sequences with reference sequence hit

163 below 90% were called unclassified.

164 Meta communities were created by combining OTU libraries of S1, S2 and S3 reactors and adding into

165 the OTU tables of original and subsampled further to the lowest sample size. α -diversity of OTU

166 libraries was measured using the Chao1, Shannon, and ACE metrics as implemented in R using

167 Phyloseq package. Microbial evenness was estimated as H_1/H_0 as described in Johnson et al. (2015a).
 168 Distance matrices were constructed using the Bray-Curtis algorithms in R. Moving windows analysis
 169 was implemented using the microbial community of the inoculum as the reference point as described in
 170 Marzorati et al. (2008). Most abundant taxa and enriched taxa in S and U reactors were visualized
 171 using the Pheatmap package in R. The 100 most abundant taxa within the samples taken at 218, 300,
 172 434, 471 days of operation were selected and compared.

173

174 **2.4 Denitrification in continuous-flow and batch experiments**

175 During continuous-flow operation, overall denitrification performance in the two MBBR systems was
 176 assessed by calculating (i) COD removal rate r_{COD} ($\text{gCOD m}^{-2} \text{d}^{-1}$) normalized per available surface
 177 area (Table S1) in each reactor, based on measured influent and effluent COD concentration in each
 178 stage; (ii) the denitrification rate normalized to surface area of reactor $r_{\text{NO}_x\text{-N}}$ ($\text{gN m}^{-2} \text{d}^{-1}$), based on the
 179 measured influent and effluent concentration of $\text{NO}_x\text{-N}$ (accounting for both $\text{NO}_3\text{-N}$ and $\text{NO}_2\text{-N}$; Sözen
 180 et al., 1998) in each stage. Measurements were taken semi-weekly during the first 100 days of
 181 operation to ensure stable start-up of the systems and semi-monthly subsequently.

182 During batch experiments, biomass-specific denitrification rates k_{NO_x} ($\text{mgN g}^{-1} \text{d}^{-1}$) were derived
 183 through linear regression of $\text{NO}_x\text{-N}$ utilization curves for each sub-stage MBBR (Polesel et al., 2017).

184 Specific denitrification rate at system level in S was calculated according to Eq. 1:

$$185 \quad k_{\text{NO}_x, S} = \frac{k_{\text{NO}_x, S1} * X_{S1} * V_{S1} + k_{\text{NO}_x, S2} * X_{S2} * V_{S2} + k_{\text{NO}_x, S3} * X_{S3} * V_{S3}}{\sum X_{\text{SMBBR}} * V_S} \quad (\text{Eq.1})$$

186 Where $k_{\text{NO}_x, S1}$, $k_{\text{NO}_x, S2}$, $k_{\text{NO}_x, S3}$, ($\text{mgN g}^{-1} \text{d}^{-1}$) indicate specific denitrification rates in S1, S2 S3
 187 respectively. X (g L^{-1}) and V (L) at the nominator in Eq. 1 indicate the biomass concentration and the

188 volume of each MBBR stage, respectively, while X_{SMBBR} (g L^{-1}) and V_{S} (L) at the denominator are the
189 biomass and volume of the staged system as a total MBBR (S).

190

191 **2.5 Micropollutants in continuous-flow and batch experiments**

192 Only indigenous pharmaceuticals occurring in municipal wastewater were quantified, as no reference
193 pharmaceuticals were spiked during continuous-flow and batch experiments. Twenty-three
194 pharmaceuticals were targeted and can be grouped in five categories: beta-blockers, sulfonamide
195 antibiotics, anti-inflammatory drugs, psycho-active drugs, X-ray contrast media. The complete list of
196 targeted pharmaceuticals quantified using HPLC-MS/MS analysis is reported in section S2 of the
197 Supplementary Information.

198 Continuous-flow samples were taken in two separate monitoring campaigns before the execution of
199 Batch 1 (100 days) and 2 (471 days) experiments. Removal efficiencies were calculated by measuring
200 influent and effluent concentration in the two systems (Polesel et al., 2017).

201 During batch experiments three main micropollutant removal mechanisms were observed or
202 hypothesized: (1) biotransformation, (2) retransformation to parent compounds (e.g., deconjugation),
203 and (3) enantioselective biotransformation (Ribeiro et al., 2013). Pseudo first-order transformation
204 kinetics k_{Bio} ($1, \text{L g}^{-1} \text{d}^{-1}$), retransformation rates k_{Dec} ($2, \text{L g}^{-1} \text{d}^{-1}$), biotransformation rate constant of
205 enantiomer 1 and 2, $k_{\text{bio},1}$ and $k_{\text{bio},2}$, ($3, \text{L g}^{-1} \text{d}^{-1}$) were estimated as described in Polesel et al. (2017)
206 using the Activated Sludge Model framework for Xenobiotics (ASM-X), accounting for sorption
207 processes (Plósz et al., 2012).

208 Subsequently, the estimated k_{Bio} and k_{Dec} in each sub-reactor of the staged MBBR configuration (Table
209 S3) were used to calculate the following kinetic parameters:

210 (i) system-level biotransformation/retransformation rate for S for each micropollutant. As
 211 described for specific denitrification rate (Eq. 1), system-level $k_{\text{Bio},S}$ (and similarly $k_{\text{Dec},S}$)
 212 were calculated according to Eq. 2:

$$214 \quad k_{\text{Bio},S} = \frac{k_{\text{Bio},S1} * X_{S1} * V_{S1} + k_{\text{Bio},S2} * X_{S2} * V_{S2} + k_{\text{Bio},S3} * X_{S3} * V_{S3}}{\sum X_{\text{SMBBR}} * V_S} \quad (\text{Eq.2})$$

215 (ii) collective rate constants of multiple pharmaceuticals (*collective* $k_{\text{Bio}S1}$ - $k_{\text{Dec}S1}$, $k_{\text{Bio}S2}$ - $k_{\text{Dec}S2}$,
 216 $k_{\text{Bio}S3}$ - $k_{\text{Dec}S3}$, $k_{\text{Bio}U}$ - $k_{\text{Dec}U}$) to compare the performance of each sub-stage of S MBBR with U
 217 MBBR in terms of micropollutant biotransformation. The rate *collective* rate constants of
 218 multiple pharmaceuticals were calculated using the multifunctionality measure described by
 219 Zavaleta et al. (2010) and Johnson et al. (2015a). Briefly, the rate constants of each
 220 pharmaceuticals were scaled (to a mean of 0, standard deviation of 1) and the *collective* rate
 221 constants were obtained by averaging of the scaled rates.

223 2.6 Analytical methods

224 In all batch and continuous-flow samples, concentrations of conventional pollutants, i.e. $\text{NO}_3\text{-N}$, $\text{NO}_2\text{-N}$,
 225 $\text{NH}_4\text{-N}$, total and soluble COD (sCOD) were measured with Hach-Lange/Merck colorimetric kits
 226 followed by spectrophotometry, as previously described in Polesel et al. (2017). Wastewater
 227 fractionation and quantification of the organic carbon availability (mg L^{-1} of biodegradable COD with
 228 its two sub-fractions, i.e., readily (Ss) and slowly (Xs) biodegradable COD) was performed according
 229 to Roeleveld and Van Loosdrecht (2002) by combination with BOD-analysis and measure of total and
 230 soluble COD. Samples for micropollutants were analyzed using HPLC-MS/MS as described in Escolà
 231 Casas et al. (2015) and in Polesel et al., (2017). Briefly, 4 mL of aqueous samples were sampled and

232 stored in glass vials with addition of 1.4 mL pure methanol (99.9%, Merck Millipore). Samples were
233 frozen at -20 °C prior analysis. For the analysis 1.5 mL of each sample were transferred to an HPLC
234 vial and centrifuged (6000 rpm, 10 min). Subsequently, 100 µL of internal standard solution was added
235 to 900 µL of the centrifuged samples solution. Samples were analyzed with an injected volume of 100
236 µL. Information regarding targeted micropollutants, HPLC-MS/MS and mass spectrometry conditions,
237 limit of quantification and detection are shown in Escolà Casas et al. (2015).

238

239 **2.7 Statistical analysis.**

240 Correlation between k_{Bio} , k_{Dec} , *collective* rate constants $k_{\text{Bio}-k_{\text{Dec}}}$ and denitrification rates k_{NO_x} ,
241 biodiversity indices (Shannon, ACE, Chao and evenness indices), denitrifying gene abundance were
242 estimated using Graph Prism 5.0. The statistical methods comprise (i) one way analysis of variance
243 (ANOVA) with Bonferroni post-hoc test (significance level at $p < 0.05$); (ii) Pearson correlation analysis
244 (r values reported) and adjusted p -values (two-tailed), and (iii) paired Wilcoxon test. Although the
245 Wilk-Shapiro test of normality may suggest a normal distribution ($p < 0.05$) as the underlying
246 distribution for the obtained biotransformation rate constants, bias could occur due to the small sample
247 size (equal to 4). Pearson coefficients were reported as an indication of the strength of the association
248 between the targeted parameters and micropollutant biotransformation rate constants.

3. Results and discussion

3.1 Comparison of continuous-flow operation performance in S and U MBBR systems

3.1.1. Denitrification

The loading of readily biodegradable (S_S) and slowly biodegradable (X_S) COD fractions in influent wastewater varied significantly through the experimental time (Fig. S2), with X_S typically contributing to more than 50% of biodegradable COD (bCOD). Most of influent S_S was utilized in the first stage S1 (on average 70%, Fig. S3a), leading to lower carbon loadings in the following stages (1.6 ± 0.4 , 0.78 ± 0.2 , 0.6 ± 0.2 gCOD d⁻¹ in S1, S2, S3 respectively, Polesel et al., 2017). A decrease in the surface-normalized COD removal rates (r_{COD} , gCOD d⁻¹ m⁻²) could be observed after approximately 70 days of operation for the three-stage and the single-stage MBBR, due to differences in carbon loading (Fig. S2). No major differences in COD removal were observed between the two systems (Fig. 1a, (iii) $p=0.46$ with Wilcoxon test), with the exception of 3 sampling days when r_{COD} was up to 2-fold higher in the three-stage MBBR. Higher variability of performance was observed in terms of NO_x-N removal in the two systems (Fig. 1b). The three-stage MBBR generally outperformed the single-stage system (up to 30% higher, for ~60% measurements) in terms of $r_{\text{NO}_x\text{-N}}$ after 50 days of operation, however the difference was found statistically insignificant ($p=0.07$, Wilcoxon test). Fluctuations in $r_{\text{NO}_x\text{-N}}$ were also caused by the variance in the influent bCOD. Biomass concentration rapidly increased in the first 100 days of operation (Fig. S4), reaching values (average \pm standard deviation) of 4.9 ± 0.9 , 5.2 ± 1.9 , 4.7 ± 1.2 , 4.47 ± 1.3 g L⁻¹, for S1, S2, S3 and U, respectively.

Overall, data during continuous-flow operation suggest an enhancement in denitrification performance in the three-stage MBBR, possibly explained based on reaction kinetics principles (Plósz, 2007), e.g.,

271 maximization of the uptake rate of S_S and less degradable organic carbon in the stages of S
272 configuration. Additionally, differences in nitrogen oxide reduction with a similar COD utilization
273 were also observed during batch experiments, resulting in different calculated observable yield $Y_{H,obs}$
274 (mgCOD mgCOD^{-1}) in the four MBBRs (Polesel et al., 2017).

275

276 <Fig.1 >

277

278 **3.1.2 Micropollutant removal**

279 During continuous-flow operation, 11 of the 23 targeted compounds were detected in the pre-clarified
280 wastewater, including compounds such as atenolol, citalopram, diclofenac, sulfamethoxazole,
281 erythromycin and iohexol (Fig. 1 c, d). During the two sampling campaigns (at ~100 and 470 days of
282 operation), atenolol and citalopram exhibited the highest removal efficiency (72% and 56–67%,
283 respectively, calculated according to Eq. S1), while the overall balance of sulfamethoxazole removal
284 showed a net formation of parent chemicals ($> -150\%$) as a results of de-conjugation of human
285 metabolites (Polesel et al., 2017). Overall, the removal efficiency of the measured pharmaceuticals was
286 not significantly different between U and S MBBR system in the two sampling campaigns ($p>0.05$,
287 Wilcoxon test in Fig. 1c and d), while diclofenac (DCF) presented higher removal in U (~10%)
288 compared to S (~20%).

289

290 **3.2 Microbial community composition and diversity in S and U MBBR systems**

291 **3.2.1 Microbial diversity at local and system level**

292 Microbial diversity in the two MBBR systems was assessed at 93%, 95%, 97% and 99% sequencing
293 similarities cut-offs to maximize the resolution of the α -diversity analysis between the four reactors.

294 After the implementation of quality control measures, a total of 3178345 high quality sequences were
295 obtained for each clustering, subsequently rarefied to 15800 sequences per sample.

296 α -diversity (expressed as Shannon diversity, ACE and Chao richness indices) increased overall with
297 increasing sequence similarity cut-offs (Fig. 2), as expected (Birtel et al., 2015). As the two MBBR
298 systems followed similar patterns over the time in terms of community diversity (Fig. 2), the α -
299 diversity was likely influenced by variations in influent wastewater composition in terms of COD and
300 microbial community in the influent wastewater, as result of frequent change of the influent medium.

301 Accordingly, linear regression analysis (Fig. S5) suggested a significant ($p < 0.05$, ANOVA) positive
302 linear relationship between influent soluble COD with microbial richness (ACE and Chao) in U (R^2 of
303 0.88, $n=6$) and S1 (R^2 of 0.80, $n=6$) at 99% similarity, but not for S, S2 and S3.

304 <Fig.2>

305 No major differences were observed in terms of Shannon diversity and evenness indices over time
306 between S and U (Fig. 2), while ACE and Chao richness presented overall higher values in S compared
307 to U (with increasing differences at increasing sequences similarity cut-offs, from 23% to 30% for 93%
308 and 99, respectively).

309 Furthermore, we assessed how the difference in the microbial community diversity in S and U (β -
310 diversity) changed over the duration of the experiment and estimated the time needed for the MBBR
311 microbial communities to reach a steady composition that was dissimilar from the inoculum (Fig. 3).

312 Moving window analysis (MWA) was implemented using the reciprocal of Bray-Curtis indices
313 measured at different sequence similarities (Fig. 3). Microbial community similarity significantly
314 decreased from the same inoculum sample during the first 200 days of operation, subsequently,
315 reaching a relatively stable composition for the rest of the experiment. Bray-Curtis indices profiles
316 (Fig. 3) for S and U decreased to the highest extent at 99% sequence similarity cut-off.

317 As the MBBR microbial communities and the degree of dissimilarity from the inoculum community
318 appeared stable after approximately 200 days of operation based on MWA, the Shannon, richness and
319 evenness indices were averaged after 200 days of operation (n=4) to assess statistical difference
320 between the two systems and for each sub-stage of S (Fig. 4). For all four tested sequence similarity
321 levels, no significant difference was observed for the Shannon diversity and evenness for the microbial
322 communities prevailing in S and U (reported at 97 and 99%, Fig. 4a–b). On the other hand, microbial
323 richness (ACE and Chao) was higher in S than to U at both sequence similarities (at system level), with
324 significant difference at 99% sequence similarity cut-off (ANOVA, $p < 0.05$, Fig. 4d).

325 <Fig.3>

326 Hence, our findings (Fig. 2 and Fig. 4) suggest that the exposure of microbial communities to a
327 gradient of organic carbon availability, achieved through reactor staging, results in significantly higher
328 microbial richness compared to a single-stage configurations. Additionally, average Shannon diversity,
329 evenness and richness were higher (although not significantly different, ANOVA, $p > 0.05$) in S3
330 compared to S1 and S2 at 99% sequence similarity (Fig. 4). It is likely that the more refractory and
331 slowly biodegradable carbon, to which S3 was exposed during continuous-flow operation (Fig. S3), led
332 to the co-existence of a more diverse microbial community due to substrate competition (Huston,
333 1994). On the contrary, the easily degradable carbon mostly utilized in S1 may have favoured
334 microbial groups that dominate the microbial community.

335 Similar observations were previously reported in managed aquifer recharge systems (MAR), where
336 higher community diversity was observed at more oligotrophic depths compared to the depths where
337 more easily degradable carbon was available (Li et al., 2013, 2012). Increased taxonomic richness was
338 also associated with lower influent ambient nitrogen and carbon availability in full-scale wastewater
339 treatment plant microbial communities (Johnson et al., 2015b). Conversely, higher microbial diversity

340 (expressed as Shannon index) was found in the first stage of an aerobic two-stage nitrifying MBBR
341 treating landfill leachate (Ciesielski et al., 2010).

342 <Fig.4>

343 **3.2.2 Temporal variability in the selection of taxa by substrate availability in S and U MBRR systems**

344 We further investigated the development of microbial structure in S and U over 471 days of operation
345 to elucidate whether staging the MBBR system resulted in a selection of specific taxa. Hence, we
346 computed heatmaps of the 100 most abundant OTUs at order level sorted by most abundant OTUs after
347 200 days of operation (218, 300, 434, 471 days) (Fig. 5 (a) and (b)). In both systems, the methanol-
348 utilizing bacteria *Methylophilales* that were enriched in the inoculum (methanol dosing was applied to
349 full-scale WWTP) decreased over time, eventually disappearing after approximately 200 days. A core
350 of OTUs was shared in both systems, consisting of *Burkholderiales*, *Xanthomonadales*,
351 *Flavobacteriales* and *Sphingobacteriales*. *Burkholderiales* (isolated from different environmental
352 sources) has been shown to be able to biotransform a vast array of aromatic compounds (Pérez-Pantoja
353 et al., 2012), as well as to be enriched by using methanol as carbon source (Kalyuzhnaya et al., 2008).
354 Bacterial strains affiliated to the order *Burkholderiale*, *Xanthomonadales* and *Sphingobacteriales* were
355 previously identified in a four-stage MBBR with a pre-denitrification configuration (Villemur et al.,
356 2015) and they were suggested to play an important role in the biofilm development, due to excretion
357 of exopolymeric substances (EPS) for biofilm formation (Pal et al., 2012). *Flavobacteriales* and
358 *Burkholderiales* were associated to the biotransformation of venlafaxine and ranitidine, respectively, in
359 WWTP community (Helbling et al., 2015). Notably, taxa such as *AKYG1722*, *Caldilineales*, *JG30-KF-*
360 *CM45* and *Candidate division WS6* were enriched in both MBBR systems during 300 days of
361 operation. To effectively identify the microbial organisms that were differently selected in the two

362 configurations, we considered the most abundant OTUs of S and U MBBRs and reported the log of the
363 ratio of the sequence abundance in S and U ($\log(S/U)$) (Fig. 5 (c)). A similar approach was used for the
364 taxa in S3 and S1 ($\log(S3/S1)$, Fig. 5 (d)). Notably, the three-stage MBBR (S) selected for the OTU
365 *Bifidobacteriales* and *Candidate division WS6* after day 218. *Candidate division WS6* have been
366 previously identified as abundant community members in anoxic/anaerobic environments of
367 hydrocarbon-and chlorinated-solvent-contaminated aquifer (Dojka et al., 1998, 2000). *Candidate*
368 *division WS6* and *Deinococcales* were enriched in S3 over S1 (Fig. 5 (4)), suggesting a correlation of
369 these OTUs with low readily biodegradable carbon availability in S3 during continuous-flow operation.
370 This is in disagreement with Dojka et al. (2000) that observed *Candidate division WS6* mainly in
371 organic-rich, anaerobic redox environment. The family *Deinococcaceae* is widely studied, since
372 organisms from this groups have been observed to exhibit remarkable resistance to radiation
373 (Chaturvedi and Archana, 2012). Conversely, *Dictyoglomales*, *Microgenomates_4* and subgroup 4 of
374 *Acidobacteria* were mostly enriched in U over S after 218 days (Fig. 5 (3)). Compared to other
375 subgroups, the abundance of *Acidobacteria subgroup 4* has been negatively associated with organic
376 carbon availability and C-to-N ratio in grassland soils (Naether et al., 2012).

377 Overall, we observed generally dynamic microbial communities, with only few taxa consistently
378 enriched after 218 days in the three-stage configuration compared to single-stage one. Considering the
379 long-term operation of the two systems with actual pre-clarified wastewater influent, it is likely that
380 (besides the organic substrate availability) continuous and random immigration by the microbial
381 community present in the influent wastewater played an important role in shaping the microbial
382 communities. The importance of microbial immigration was shown by calibrating a neutral model
383 community assembly with dynamic observations of wastewater treatment communities (Ofiteru et al.,
384 2010), in full-scale WWTP (Wells et al., 2014), as well as in a pilot-scale membrane bioreactor system

385 (Arriaga et al., 2016). Additionally, cross-inoculation between staged reactors may have been occurred,
386 as previously observed in staged bioprocesses in full-scale WWTP (Wells et al., 2014).

387 <Fig. 5>

ACCEPTED MANUSCRIPT

388 3.2.3 Microbial and denitrifying gene abundance in S and U MBBR systems

389 Quantification of 16S rRNA (total bacteria) and denitrifying genes was performed to investigate
390 differences in denitrifying microbial communities in the four MBBR reactors (Fig. S6). For the U and
391 S1 MBBR, microbial abundance of total bacteria during 471 days of operation could be associated with
392 the influent substrate concentration – expressed as influent soluble COD (Fig. S7, R^2 of 0.8 and 0.5,
393 respectively). Conversely, no association was found for S2 and S3 with respect to influent sCOD.

394 As informed by moving window analysis, qPCR data for all reactors were averaged from the point
395 when the microbial community was stable (i.e., after 200 days of operation) (Table 1). The lowest
396 ($p < 0.05$) abundance of 16S rRNA gene (copies g_{biomass}^{-1}) was measured in S3, mostly adapted to carbon
397 limitation during continuous-flow operation, as previously observed in simulated managed aquifer
398 recharge (Li et al., 2013). Overall, the measured *nirS* gene fraction was up to 10 times higher than *nirK*
399 (in agreement with other studies in aquatic ecosystems, e.g., Braker et al., 2000;), while no differences
400 were observed between the four reactors in terms of *nirS* gene fraction (Table 1). Previous studies have
401 suggested lower densities of *nirK*-containing denitrifiers in aquatic ecosystems (Braker et al., 2000).
402 The decrease of *nirS* from the inoculum sample (day 0), adapted to methanol (Fig. S6) is consistent
403 with the previous observation that utilization of methanol as a readily biodegradable substrate can
404 select for *nirS*-expressing denitrifiers (Hallin et al., 2006). Furthermore, a change to different carbon
405 sources can result in a loss of *nirS* density (Hallin et al., 2006). The S3 reactor was continuously
406 exposed to the lowest C-to-N influent ratio (average values of C, expressed as sCOD, -to-N ratio of 1,
407 0.8 and 0.7 for S1 and U, S2, S3 respectively), and previous research reported increased N_2O
408 production at lower C-to-N ratios (Zhang et al., 2016). However, S3 exposed to lower C-to-N ratios
409 during continuous-flow operation exhibited the highest ($p < 0.05$) abundance of atypical *nosZ* gene and a

410 lower nitrite reductase and nitrous reductase ration (Table 1), which could indicate a more effective
411 N₂O removal with respect to other reactor stages. Furthermore, S3 and S1 had the highest and lowest
412 ratio of atypical to typical *nosZ*, respectively (Table 1). Typical *nosZ* genes have been associated with
413 bacteria capable of complete denitrification (thus encoding all the enzymes for converting nitrate to
414 nitrogen) (Sanford et al., 2012). In contrast, atypical *nosZ* genes were also found in non-denitrifying
415 bacteria with more-diverse N-metabolism (e.g., missing *nirK* and *nirS*) (Orellana et al., 2014; Sanford
416 et al., 2012), and are commonly present at concentrations higher than typical *nosZ* in soil (Orellana et
417 al., 2014). Hence, our results suggest a microbial selection driven by the substrate gradient through the
418 MBBR stages, where most of the complete denitrifiers (carrying typical *nosZ*) are selected in S1 (with
419 the highest readily biodegradable substrate availability). On the other hand, microbes with more diverse
420 N-metabolism (carrying atypical *nosZ*) are selected in S3. Although, based on prior reports, the highest
421 N₂O production was expected in MBBR stages with low influent C-to-N ratio, the selection of non-
422 denitrifying bacteria containing atypical *nosZ* genes (which code for high affinity N₂O reductase) may
423 well imply a reduced accumulation of nitrous oxide. This factor suggests biofilm reactor staging as a
424 process optimisation means to reduce N₂O emissions through wastewater treatment, which requires
425 further research.

426
427 <Table 1>
428
429
430
431

432 **3.3. Linking activity, community composition and diversity with micropollutant**
433 **biotransformation in batch experiments**

434

435 **3.3.2 System level (*S* and *U*)**

436 Based on the results of the batch experiments, biotransformation rate constants of the pharmaceuticals
437 were calculated at system level for the three-stage MBBR system (Eq. 2) and compared with rate
438 constants for the single-stage system for Batch 1 (Fig. S11) and Batch 2 (Fig. 6 a). We did not observe
439 a significant difference in specific denitrification rate at system level (calculated as in Eq. 1) but higher
440 ($p < 0.05$) microbial richness was measured in *S* compared to *U* in Batch 2 (Fig. 6b). Nonetheless, no
441 significant difference was observed in the biotransformation of the targeted micropollutants between
442 the two MBBR systems (Fig S11 and Fig. 6a).

443

<Fig. 6>

444

445 **3.3.1. Local level (*S1*, *S2*, *S3* and *U*)**

446 As reported in Polesel et al., 2017, the decreasing loading and availability of carbon during
447 continuous-flow operation led to a decreasing trend of pharmaceuticals biotransformation from *S1* to
448 *S3* (Table S3).

449 Pearson's coefficients r were used to evaluate associations between biotransformation rate constant k_{Bio}
450 / k_{Dec} and (i) biodiversity indices (at 99% sequence similarity, Fig. S9); (ii) denitrifying gene abundance
451 (Fig. S6); (iii) specific denitrification rates \bar{k}_{NOX} ($\text{mgN g}^{-1} \text{d}^{-1}$) (Table S3). Only relevant k_{Bio} and k_{Dec}
452 values ($>0.1 \text{ L g}^{-1} \text{d}^{-1}$ and corresponding to a removal $>20\%$ according to the classification presented in
453 Joss et al., 2006) were included in the analysis. Notably, correlations were performed by using only
454 taxonomic diversity (based on 16S rRNA amplicon sequencing), rather than data combining functional

455 diversity (based on the phenotypes inferred from taxonomic descriptors and on mRNA sequencing),
456 which was beyond the scope of this study. Although it has been observed that taxonomic and functional
457 diversity associate with each other in wastewater treatment systems (Johnson et al., 2015b), additional
458 information could be derived by the combination of both analyses.

459 In Batch 1, only few positive correlations ($p < 0.05$) were observed between diversity indices and
460 biotransformation rate constants of pharmaceuticals. i.e., sulfamethoxazole, trimethoprim and
461 metoprolol (Fig. S10). In Batch 2, k_{Bio} and k_{Dec} of most detected pharmaceuticals were negative or not
462 significantly correlated with microbial richness (Fig. 7), but positively correlated ($p < 0.05$) with specific
463 denitrification rates k_{NO_x} . The obtained correlations are reported in Fig. S8. Positive correlations
464 ($p < 0.05$) were found with k_{Bio} of erythromycin, trimethoprim and *collective* pharmaceuticals as well as
465 with the abundance of denitrifying genes *narG*, *nirS*, and *nosZ* typical, but not atypical *nosZ*.

466 The difference in the results between Batch 1 and 2 may stem from the variation in the denitrification
467 rates k_{NO_x} obtained during batch experiment, that affected the cometabolic biotransformation of the
468 pharmaceuticals (Polesel et al., 2017). Due to lower biotransformation rate constants obtained in Batch
469 2 compared to Batch 1, adaption of the biomass to targeted pharmaceuticals is unlikely. Previous
470 studies on soil and wastewater activated sludge concluded that pre-exposure of the biomass to trace
471 organic chemicals may not affect the removal efficiency of micropollutants (Falås et al., 2016) neither
472 the microbial community structure nor its function (analyzed by metagenomes) (Alidina et al., 2014).

473 As discussed previously, a stable microbial community was observed only after 200 days of operation
474 and results from Batch 2 (at 471 days) may be considered representative of the long-time operation of
475 the two MBBR systems.

476 Biotransformation of several micropollutants has been related to the lack of specificity of enzymes such
477 as ammonia monooxygenase (Khunjar et al., 2011; Sathyamoorthy et al., 2013). To our knowledge,

478 cometabolism of micropollutants by respiratory denitrifying enzymes (e.g., *narG*, *nirS*, *nor*, *nosZ*) has
479 not been documented. Thus, the unexpected association between denitrifying genes and
480 biotransformation of micropollutants may be the result of a genuine but nevertheless non-causal
481 relationship (Johnson et al., 2015c). Further research is required to examine the cause of this
482 correlation.

483 As mentioned previously, positive relationships between microbial diversity (and in particular α -
484 diversity) and biotransformation rate constants of micropollutants have been observed in activated
485 sludge (Johnson et al., 2015a), in sequencing batch lab-reactors (Stadler and Love, 2016) and in
486 nitrifying MBBRs (Torresi et al., 2016). Yet, similar negative correlation has been observed between
487 biodiversity and removal of natural and synthetic estrogens in suspended biomass (Pholchan et al.,
488 2013; Tan et al., 2013) and for sulfonamide antibiotics (sulfadiazine, sulfamethoxazole, sulfamethizole)
489 in nitrifying MBBRs (Torresi et al., 2016). Among others, two phenomena may explain the lack of an
490 observable (positive) relationship:

491 (i) A positive relationship between biodiversity (or richness) would emerge (a) if the microbial
492 community consisted of a number of microorganisms with unique niche partitioning or (b) if
493 facilitative interactions (i.e., complementarity effects) occurred (Cardinale, 2011) .
494 However, functional redundancy (i.e., different taxa coexist to perform the same
495 functionality) could be sufficient to mask this positive interaction (Johnson et al., 2015b).
496 Accordingly, if the biotransformation of a specific compound is performed by a large
497 number of taxa, the increase of biodiversity may not necessary positively impact the
498 biotransformation as it is not limited by the number of taxa that can perform it (Stadler and
499 Love, 2016). Taken together, the negative correlation observed in this study between
500 biotransformation rate constants and biodiversity, combined with the positive correlation

501 with kinetics of denitrification, could suggest a redundancy of the denitrifying microbial
502 community towards the biotransformation of these targeted pharmaceuticals.

503 This observation might further suggest that denitrifying systems exhibit higher
504 biotransformation rates of pharmaceuticals compared to aerobic systems, due to the higher
505 number of taxa performing this function. Hence, we compared the average
506 biotransformation rate constants obtained in this study (under pre-denitrification conditions)
507 and in post-denitrification MBBRs (Torresi et al., 2017) with kinetics obtained for aerobic
508 nitrifying MBBRs (Torresi et al., 2016) (Fig. S12). While we observed comparable
509 biotransformation kinetics for aerobic and pre-denitrifying MBBRs (this study) (Fig. S12a),
510 post-denitrifying MBBRs indeed exhibited higher biotransformation rate constants for more
511 than 60% of the examined pharmaceuticals (Fig. S12b) compared to aerobic MBBRs. In the
512 post-denitrifying MBBRs (Torresi et al., 2017), additional carbon sources (i.e., methanol or
513 ethanol) were dosed in the systems, which are known to be readily biodegradable substrates.
514 Thus, in the absence of catabolic limitation (i.e., in the presence of excess easily degradable
515 organic carbon), biotransformation of several targeted pharmaceuticals may be more
516 expedient under anoxic versus aerobic conditions.

517 (ii) An increase in biodiversity might not translate into differences in microbial functionality if
518 the microbial community presents sufficient biodiversity to begin with, that can saturate the
519 possible effects (Johnson et al 2015a). While this effect was not observed for suspended
520 biomass in full-scale WWTP (i.e., microbial communities were not sufficiently diverse to
521 maximize the collective rate of multiple micropollutant biotransformation, Johnson et al.,
522 (2015a)), this may be different for biofilm systems that can already potentially harbor higher
523 microbial diversity compared to suspended biomass (Stewart and Franklin, 2008).

524 Overall, our results (at both global and system level) suggest that despite the general positive
525 association between microbial diversity and ecological activity (Cardinale, 2011; Emmett Duffy, 2009),
526 this association is not fully understood for microbial communities in biological wastewater treatment
527 regarding micropollutant biotransformation. On the other hand, additionally information could be
528 obtained by targeting a broader number of micropollutants.

529 Nonetheless, the relationships between microbial diversity and system stability and resilience in
530 wastewater treatment plant has been discussed (Lu et al., 2014), as a result of functional redundancy
531 (Briones and Raskin, 2003). Accordingly, it has been recommended that if two denitrifying
532 configurations perform equally efficiently, the configuration with higher functional diversity should be
533 preferentially selected to ensure higher system stability (Lu et al., 2014).

534

535

536

537

538 **4. Conclusions**

539 The microbial communities of two pre-denitrifying MBBR systems operated in parallel in single- (U)
540 and three-stage (S) configurations using pre-clarified wastewater as influent and native concentration of
541 micropollutants were investigated during long-term operation.

- 542 • The decreasing gradient of organic carbon loading and availability (created through MBBR
543 staging) led to an increase of α -diversity of the microbial community (although not significant)
544 within the three-stage system and an overall increased richness (ANOVA, $p < 0.05$) of the
545 microbial community in the S configuration compared to U.
- 546 • The microbial community became stable only after 200 days of operation, when the two
547 configurations shared a core of OTUs such as *Burkholderiales*, *Xanthomonadales*,
548 *Flavobacteriales* and *Sphingobacteriales*. The staged configuration (and in particular in the last
549 stage MBBR, S3) selected for OTUs such as *Candidatus division WS6* and *Deinococcales*.
- 550 • S3 exposed to lower C-to-N ratios during continuous-flow operation exhibited the highest
551 ($p < 0.05$) abundance of atypical *nosZ* gene and a lower nitrite reductase and nitrous reductase
552 ration, suggesting a more effective N_2O removal with respect to other reactor stages.
- 553 • Specific and *collective* bio- and re-transformation rate constants of the targeted pharmaceuticals
554 positively correlated with specific denitrification rates and abundance of denitrifying genes
555 (*narG*, *nirS* and *nosZ* typical), rather than biodiversity.

556 Overall, staging of MBBR systems under denitrifying conditions resulted in enhanced denitrification
557 rate and increased microbial diversity compared to a single-stage configuration, although no major
558 improvement was observed in the removal of the selected trace organic pharmaceuticals.

559

560 **Acknowledgements**

561 This research was supported by MERMAID: an Initial Training Network funded by the People
562 Programme (Marie-Curie Actions) of the European Union's Seventh Framework Programme
563 FP7/2007-2013/under REA grant agreement n. 607492. The authors thank Luca Loreggian and Saverio
564 Conti for technical support.

565

566

567 **References**

- 568 Alidina, M., Li, D., Ouf, M., Drewes, J.E., 2014. Role of primary substrate composition and
569 concentration on attenuation of trace organic chemicals in managed aquifer recharge systems. *J.*
570 *Environ. Manage.* 144, 58–66.
- 571 Arriaga, S., De Jonge, N., Lund Nielsen, M., Andersen, H.R., Borregaard, V., Jewel, K., Ternes, T.A.,
572 Lund Nielsen, J., 2016. Evaluation of a membrane bioreactor system as post-treatment in waste
573 water treatment for better removal of micropollutants.
- 574 Barbosa, M.O., Moreira, N.F.F., Ribeiro, A.R., Pereira, M.F.R., Silva, A.M.T., 2016. Occurrence and
575 removal of organic micropollutants: An overview of the watch list of EU Decision 2015/495.
576 *Water Res.* 94, 257–279.
- 577 Birtel, J., Walser, J.-C., Pichon, S., Bürgmann, H., Matthews, B., 2015. Estimating Bacterial Diversity
578 for Ecological Studies: Methods, Metrics, and Assumptions. *PLoS One* 10.
- 579 Braker, G., Zhou, J., Wu, L., Devol, A.H., Tiedje, J.M., 2000. Nitrite reductase genes (*nirK* and *nirS*)
580 as functional markers to investigate diversity of denitrifying bacteria in pacific northwest marine
581 sediment communities. *Appl. Environ. Microbiol.* 66, 2096–104. Briones, A., Raskin, L., 2003.
582 Diversity and dynamics of microbial communities in engineered environments and their
583 implications for process stability. *Curr. Opin. Biotechnol.* 14, 270–276.
- 584 Carballa, M., Omil, F., Lema, J.M., Llompарт, M., García-Jares, C., Rodríguez, I., Gomez, M., Ternes,
585 T., 2004. Behavior of pharmaceuticals, cosmetics and hormones in a sewage treatment plant.
586 *Water Res.* 38 (12), 2918e2926.
- 587 Cardinale, B.J., 2011. Biodiversity improves water quality through niche partitioning. *Nature* 472, 86–
588 9.

- 589 Chaturvedi, R., Archana, G., 2012. Novel 16S rRNA based PCR method targeting *Deinococcus* spp.
590 and its application to assess the diversity of deinococcal populations in environmental samples. *J.*
591 *Microbiol. Methods* 90, 197–205.
- 592 Ciesielski, S., Kulikowska, D., Kaczowka, E., Kowal, P., 2010. Characterization of bacterial structures
593 in a two-stage moving-bed biofilm reactor (MBBR) during nitrification of the landfill leachate. *J.*
594 *Microbiol. Biotechnol.* 20, 1140–1151.
- 595 Dojka, M.A., Harris, J.K., Pace, N.R., 2000. Expanding the known diversity and environmental
596 distribution of an uncultured phylogenetic division of bacteria. *Appl. Environ. Microbiol.* 66,
597 1617–21.
- 598 Dojka, M., Hugenholtz, P., Haack, S., Pace, N., 1998. Microbial diversity in a hydrocarbon-and
599 chlorinated-solvent-contaminated aquifer undergoing intrinsic bioremediation. *Appl. Environ.*
600 *Microbiol.* 64, 3869–3877.
- 601 Emmett Duffy, J., 2009. Why biodiversity is important to the functioning of real-world ecosystems.
602 *Front. Ecol. Environ.* 7, 437–444.
- 603 Escolà Casas, M.E., Chhetri, R.K., Ooi, G., Hansen, K.M.S., Litty, K., Christensson, M., Kragelund,
604 C., Andersen, H.R., Bester, K., 2015. Biodegradation of pharmaceuticals in hospital wastewater
605 by staged Moving Bed Biofilm Reactors (MBBR). *Water Res.* 83, 293–302.
- 606 Falås, P., Wick, A., Castronovo, S., Habermacher, J., Ternes, T.A., Joss, A., 2016. Tracing the limits of
607 organic micropollutant removal in biological wastewater treatment. *Water Res.* 95, 240–249.
- 608 Fu, B., Liao, X., Ding, L., Ren, H., 2010. Characterization of microbial community in an aerobic
609 moving bed biofilm reactor applied for simultaneous nitrification and denitrification. *World J.*
610 *Microbiol. Biotechnol.* 26, 1981–1990.
- 611 Hallin, S., Throbäck, I.N., Dicksved, J., Pell, M., 2006. Metabolic profiles and genetic diversity of

- 612 denitrifying communities in activated sludge after addition of methanol or ethanol. *Appl. Environ.*
613 *Microbiol.* 72, 5445–5452.
- 614 Helbling, D.E., Johnson, D.R., Lee, T.K., Scheidegger, A., Fenner, K., 2015. A framework for
615 establishing predictive relationships between specific bacterial 16S rRNA sequence abundances
616 and biotransformation rates. *Water Res.* 70, 471–484.
- 617 Huston, M.A., 1994. *Biological Diversity: the Coexistence of Species*. Cambridge University Press.
- 618 Johnson, D.R., Helbling, D.E., Lee, T.K., Park, J., Fenner, K., Kohler, H.P.E., Ackermann, M., 2015a.
619 Association of biodiversity with the rates of micropollutant biotransformations among full-scale
620 wastewater treatment plant communities. *Appl. Environ. Microbiol.* 81, 666–675.
- 621 Johnson, D.R., Lee, T.K., Park, J., Fenner, K., Helbling, D.E., 2015b. The functional and taxonomic
622 richness of wastewater treatment plant microbial communities are associated with each other and
623 with ambient nitrogen and carbon availability. *Environ. Microbiol.* 17, 4851–4860.
- 624 Johnson, D.R., Helbling, D.E., Men, Y., Fenner, K., 2015c. Can 613 meta-omics help to establish
625 causality between contaminant biotransformations and genes or gene products? *Environ. Sci. Water*
626 *Res. Technol.* 1, 272–278.
- 627 Joss, A., Zabczynski, S., Göbel, A., Hoffmann, B., Löffler, D., McArdell, C.S., Ternes, T. A.,
628 Thomsen, A., Siegrist, H., 2006. Biological degradation of pharmaceuticals in municipal
629 wastewater treatment: Proposing a classification scheme. *Water Res.* 40, 1686–1696.
- 630 Kalyuzhnaya, M.G., Hristova, K.R., Lidstrom, M.E., Chistoserdova, L., 2008. Characterization of a
631 novel methanol dehydrogenase in representatives of Burkholderiales: implications for
632 environmental detection of methylotrophy and evidence for convergent evolution. *J. Bacteriol.*
633 190, 3817–23.
- 634 Khunjar, W. O.; Mackintosh, S. A.; Skotnicka-Pitak, J.; Baik, S.; Aga, D. S.; Love, N. G. Elucidating

- 635 the relative roles of ammonia oxidizing and heterotrophic bacteria during the biotransformation of
636 17alpha-Ethinylestradiol and trimethoprim. *Environ. Sci. Technol.* 2011, 45 (8), 3605–3612. (14)
- 637 Li, D., Sharp, J.O., Saikaly, P.E., Ali, S., Alidina, M., Alarawi, M.S., Keller, S., Hoppe-Jones, C.,
638 Drewes, J.E., 2012. Dissolved organic carbon influences microbial community composition and
639 diversity in managed aquifer recharge systems. *Appl. Environ. Microbiol.* 78, 6819–6828.
- 640 Li, D., Alidina, M., Ouf, M., Sharp, J.O., Saikaly, P., Drewes, J.E., 2013. Microbial community
641 evolution during simulated managed aquifer recharge in response to different biodegradable
642 dissolved organic carbon (BDOC) concentrations. *Water Res.* 47, 2421–30.
- 643 Lu, H., Chandran, K., Stensel, D., 2014. Microbial ecology of denitrification in biological wastewater
644 treatment. *Water Res.* 64, 237–254.
- 645 Marzorati, M., Wittebolle, L., Boon, N., Daffonchio, D., Verstraete, W., 2008. How to get more out of
646 molecular fingerprints: practical tools for microbial ecology. *Environ. Microbiol.* 10, 1571–81.
- 647 Naether, A., Foesel, B.U., Naegele, V., Wüst, P.K., Weinert, J., Bonkowski, M., Alt, F., Oelmann, Y.,
648 Polle, A., Lohaus, G., Gockel, S., Hemp, A., Kalko, E.K. V, Linsenmair, K.E., Pfeiffer, S.,
649 Renner, S., Schöning, I., Weisser, W.W., Wells, K., Fischer, M., Overmann, J., Friedrich, M.W.,
650 2012. Environmental factors affect Acidobacterial communities below the subgroup level in
651 grassland and forest soils. *Appl. Environ. Microbiol.* 78, 7398–406. Ofiteru, I.D., Lunn, M.,
652 Curtis, T.P., Wells, G.F., Criddle, C.S., Francis, C.A., Sloan, W.T., 2010. Combined niche and
653 neutral effects in a microbial wastewater treatment community. *Proc. Natl. Acad. Sci.* 107, 15345–
654 15350.
- 655 Orellana, L.H., Rodriguez-R, L.M., Higgins, S., Chee-Sanford, J.C., Sanford, R.A., Ritalahti, K.M.,
656 Löffler, F.E., Konstantinidis, K.T., 2014. Detecting nitrous oxide reductase (NosZ) genes in soil
657 metagenomes: method development and implications for the nitrogen cycle. *MBio* 5, e01193-14.

- 658 Painter, M.M., Buerkley, M.A., Julius, M.L., Vajda, A.M., Norris, D.O., Barber, L.B., Furlong, E.T.,
659 Schultz, M.M., Schoenfuss, H.L., 2009. Antidepressants at environmentally relevant
660 concentrations affect predator avoidance behavior of larval fathead minnows (*Pimephales*
661 *Promelas*). *Environ. Toxicol. Chem.* 28, 2677.
- 662 Pal, L., Kraigher, B., Brajer-Humar, B., Levstek, M., Mandic-Mulec, I., 2012. Total bacterial and
663 ammonia-oxidizer community structure in moving bed biofilm reactors treating municipal
664 wastewater and inorganic synthetic wastewater. *Bioresour. Technol.* 110, 135e143
- 665 Pérez-Pantoja, D., Donoso, R., Agulló, L., Córdova, M., Seeger, M., Pieper, D.H., González, B., 2012.
666 Genomic analysis of the potential for aromatic compounds biodegradation in Burkholderiales.
667 *Environ. Microbiol.* 14, 1091–1117.
- 668 Pholchan, M.K., de Baptista, J.C., Davenport, R.J., Sloan, W.T., Curtis, T.P., 2013. Microbial
669 community assembly, theory and rare functions. *Front. Microbiol.* 4, 1–9.
- 670 Plósz, B.G., 2007. Optimization of the activated sludge anoxic reactor configuration as a means to
671 control nutrient removal kinetically. *Water Res.* 41, 1763–1773.
- 672 Plósz, B.G., Langford, K.H., Thomas, K. V., 2012. An activated sludge modeling framework for
673 xenobiotic trace chemicals (ASM-X): assessment of diclofenac and carbamazepine. *Biotechnol.*
674 *Bioeng.* 109, 2757–69.
- 675 Polesel, F., Torresi, E., Loreggian, L., Casas, M.E., Christensson, M., Bester, K., Plósz, B.G., 2017.
676 Removal of pharmaceuticals in pre-denitrifying MBBR – Influence of organic substrate
677 availability in single- and three-stage configurations. *Water Res.* 123, 408–419.
- 678 Price, M.N., Dehal, P.S., Arkin, A.P., 2009. FastTree: computing large minimum evolution trees with
679 profiles instead of a distance matrix. *Mol. Biol. Evol.* 26, 1641–50.
- 680 Ribeiro, A.R., Afonso, C.M., Castro, P.M.L., Tiritan, M.E., 2013. Enantioselective HPLC analysis and

- 681 biodegradation of atenolol, metoprolol and fluoxetine. *Environ. Chem. Lett.* 11, 83e90.
- 682 Roeleveld, P.J., Van Loosdrecht, M.C.M., 2002. Experience with guidelines for wastewater
683 characterisation in The Netherlands. *Water Sci. Technol.* 45, 77–87.
- 684 Sanford, R.A., Wagner, D.D., Wu, Q., Chee-Sanford, J.C., Thomas, S.H., Cruz-García, C., Rodríguez,
685 G., Massol-Deyá, A., Krishnani, K.K., Ritalahti, K.M., Nissen, S., Konstantinidis, K.T., Löffler,
686 F.E., 2012. Unexpected nondenitrifier nitrous oxide reductase gene diversity and abundance in
687 soils. *Proc. Natl. Acad. Sci. U. S. A.* 109, 19709–14.
- 688 Sathyamoorthy S, Chandran K, Ramsburg CA (2013) Biodegradation and cometabolic modeling of
689 selected beta blockers during ammonia oxidation. *Environ Sci Technol* 47:12835–12843
- 690 Schloss, P.D., 2009. Introducing mothur: A Computational Toolbox for Describing and Comparing
691 Microbial Communities. *Abstr. Gen. Meet. Am. Soc. Microbiol.* 109.
- 692 Stadler, L.B., Love, N.G., 2016. Impact of microbial physiology and microbial community structure on
693 pharmaceutical fate driven by dissolved oxygen concentration in nitrifying bioreactors. *Water Res.*
694 104, 189–199.
- 695 Stewart, P.S., Franklin, M.J., 2008. Physiological heterogeneity in biofilms. *Nat Rev Micro* 6, 199–
696 210.
- 697 Sözen, S., Çokgör, E.U., Orhon, D., Henze, M., 1998. Respirometric analysis of activated sludge
698 behaviour—II. Heterotrophic growth under aerobic and anoxic conditions. *Water Res.* 32, 476–
699 488.
- 700 Tan, D.T., Arnold, W.A., Novak, P.J., 2013. Impact of organic carbon on the biodegradation of estrone
701 in mixed culture systems. *Environ. Sci. Technol.* 47, 12359–12365.
- 702 Torresi, E., Fowler, J.S., Polesel, F., Bester, K., Andersen, H.R., Smets, B.F., Plosz, B.G.,
703 Christensson, M., 2016. Biofilm thickness influences biodiversity in nitrifying MBBRs –

- 704 Implications on micropollutant removal. *Environ. Sci. Technol.* 50, 9279–9288.
- 705 Torresi, E., Casas, M.E.C., Polesel, F., Pl, B.G., Bester, K., 2017. Impact of external carbon dose on the
706 removal of micropollutants using methanol and ethanol in post-denitrifying moving bed biofilm
707 reactors 108, 95–105.
- 708 Villemur, R., Juteau, P., Bougie, V., Ménard, J., Déziel, E., 2015. Development of four-stage moving
709 bed biofilm reactor train with a pre-denitrification configuration for the removal of thiocyanate
710 and cyanate. *Bioresour. Technol.* 181, 254–262.
- 711 Wells, G.F., Wu, C.H., Piceno, Y.M., Eggleston, B., Brodie, E.L., DeSantis, T.Z., Andersen, G.L.,
712 Hazen, T.C., Francis, C.A., Criddle, C.S., 2014. Microbial biogeography across a full-scale
713 wastewater treatment plant transect: Evidence for immigration between coupled processes. *Appl.*
714 *Microbiol. Biotechnol.* 98, 4723–4736.
- 715 Xia, S., Li, J., Wang, R., Li, J., Zhang, Z., 2010. Tracking composition and dynamics of nitrification
716 and denitrification microbial community in a biofilm reactor by PCR-DGGE and combining FISH
717 with flow cytometry. *Biochem. Eng. J.* 49, 370–378.
- 718 Yu, Y., Lee, C., Kim, J., Hwang, S., 2005. Group-specific primer and probe sets to detect
719 methanogenic communities using quantitative real-time polymerase chain reaction. *Biotechnol.*
720 *Bioeng.* 89, 670–9.
- 721 Zavaleta, E.S., Pasari, J.R., Hulvey, K.B., David Tilman, G., 2010. Sustaining multiple ecosystem
722 functions in grassland communities requires higher biodiversity. *Proc. Natl. Acad. Sci.* 104, 1443–
723 1446.
- 724 Zhang, Y., Ji, G., Wang, R., 2016. Drivers of nitrous oxide accumulation in denitrification biofilters
725 with low carbon:nitrogen ratios. *Water Res.* 106, 79–85.
- 726 Ødegaard, H., 1999. The Moving Bed Biofilm Reactor. *Water Environ. Eng. Reuse Water* 250–305.

727 **Tables**

728

729 **Table 1.** Results from qPCR targeting 16S rRNA and functional genes in the four MBBRs (S1, S2, S3, U).

730 Values result from the average of the last four sampling days (218, 300, 434 and 471) after microbial community

731 stabilization according to MWA. Values are reported with the corresponding standard deviation (n=8). Statistical

732 differences ($p < 0.05$) were estimated according to one way analysis (ANOVA).

	S1	S2	S3	U
16S rRNA	$2.13 \times 10^{11} \pm$	$1.57 \times 10^{11} \pm$	$7.24 \times 10^{10} \pm$	$2.2 \times 10^{11} \pm$
(copies/g _{biomass})	44%	16%	7% ⁽¹⁾	19%
<i>narG</i> (%)*	48 ± 20	22 ± 7 ⁽²⁾	53 ± 22	27 ± 9
<i>nirS</i> (%)*	58 ± 10	54 ± 9	63 ± 6	64 ± 9
<i>nirK</i> (%)*	8 ± 4	12 ± 7	11 ± 5	11 ± 7
<i>nirS/nirK</i>	6.9 ± 3	8.3 ± 3	6.3 ± 3	10.9 ± 11
<i>nosZ_{typ}</i> (%)*	9 ± 3	9 ± 1	9 ± 1	9 ± 2
<i>nosZ_{atyp}</i> (%)*	6 ± 1	8 ± 5	15 ± 8 ⁽³⁾	11 ± 5
<i>nosZ_{atyp}/nosZ_{typ}</i>	0.72 ± 0.23	0.93 ± 0.53	1.60 ± 0.71 ⁽³⁾	1.36 ± 0.62
<i>(nirK+nirS)/</i> <i>(nosZ_{atyp}+nosZ_{typ})</i>	4.68+1.14 ⁽⁴⁾	3.86+0.59	3.51+1.11	3.96+0.70

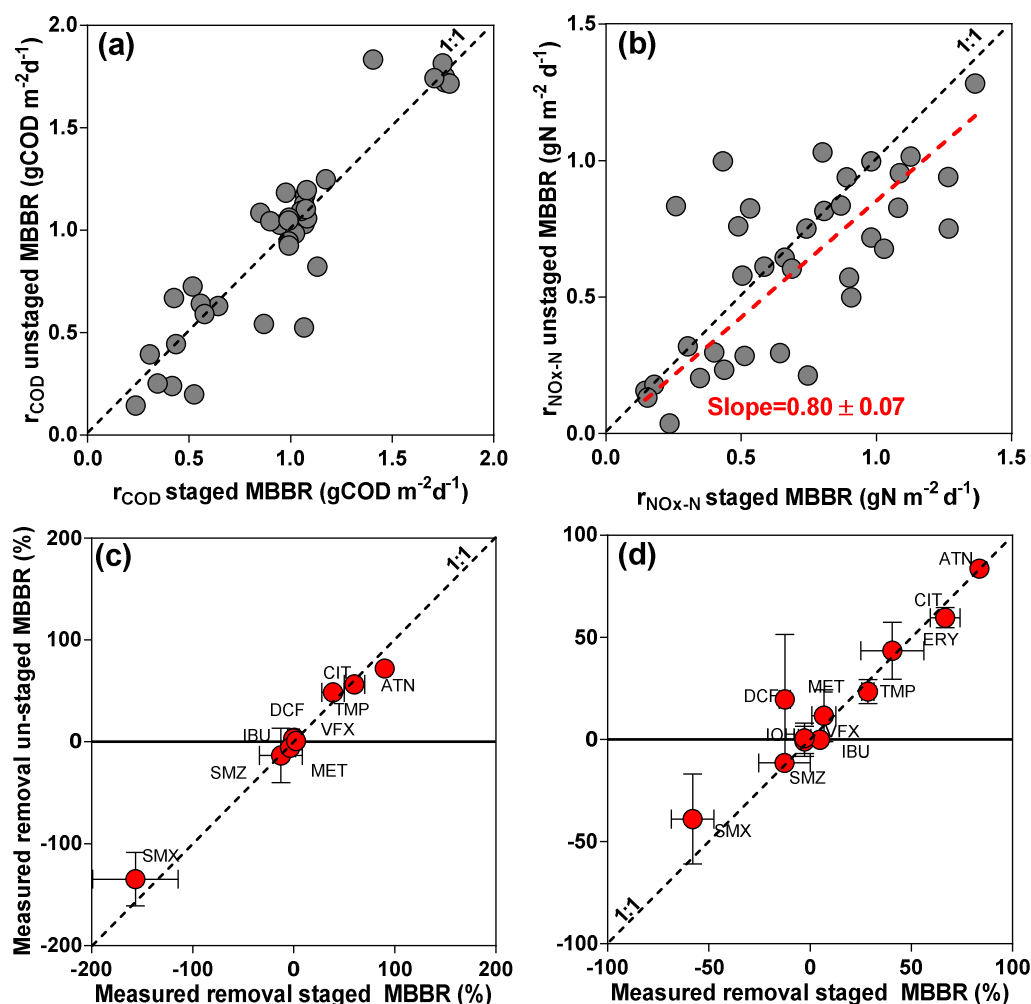
733 * % of 16S rRNA gene abundance

734

734 ⁽¹⁾ significantly lower than S1 and U (95% confidence interval)735 ⁽²⁾ significantly lower than S1 and S3 (95% confidence interval)736 ⁽³⁾ significantly higher than S1 and S2 (95% confidence interval)

737 ⁽⁴⁾ significantly higher than S3 (95% confidence interval)

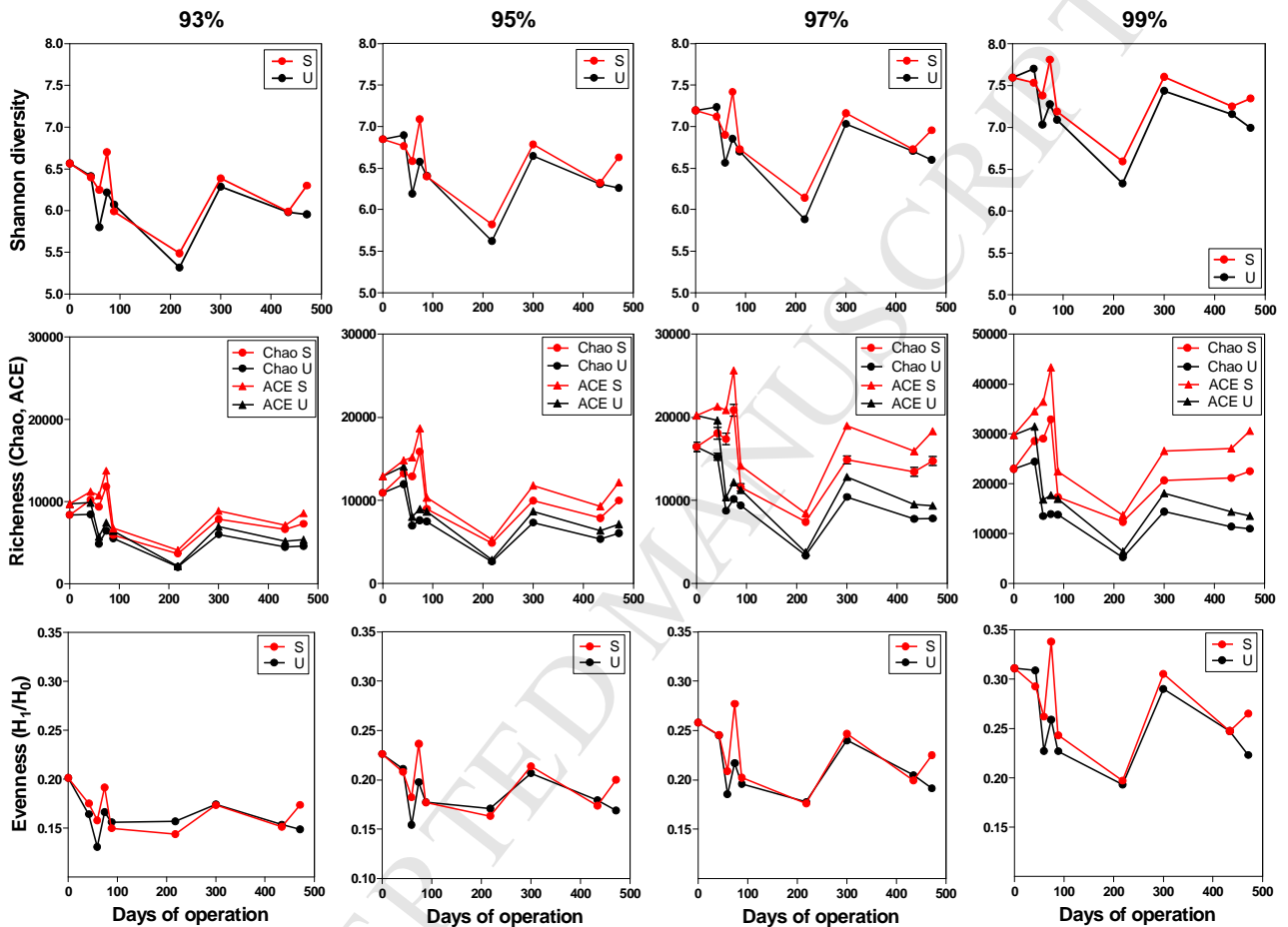
738 **Figures**



739

740 **Figure 1.** Measured data from continuous-flow operation. Comparison between COD removal rates (r_{COD} ,
 741 gCOD d⁻¹ m⁻²) (a) and denitrification rate ($r_{\text{NOx-N}}$, gN m⁻² d⁻¹) (b) in the three-(S) and single-stage (U) MBBR
 742 configuration (n=40); comparison between micropollutant removal (%) in S and U in the first (c, ~100 days of
 743 operation) and second (d, ~470 days of operation) campaigns (Polesel et al., 2017). Dashed red line in (b) shows
 744 linear regression (slope 0.80 ± 0.07 , $p < 0.001$). Abbreviations: ATN = atenolol; CIT = citalopram; TMP =

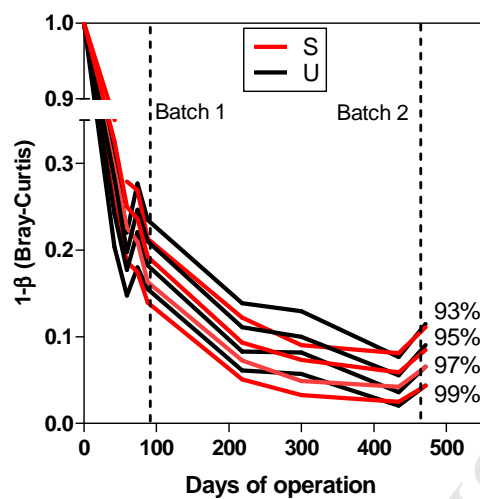
745 trimethoprim; DCF = diclofenac; IBU= ibuprofen; MET = metoprolol; SMX = sulfamethoxazole; SMZ =
 746 sulfamethizole; VFX = venlafaxine; ERY = erythromycin; IOH = iohexol.



747
 748

749 **Figure 2.** Shannon, richness (Chao and ACE) and evenness (H_1/H_0) indices measured at different time points for
 750 the three-(S) and single-stage (U) MBBR configuration at 93, 95, 97 99% of sequencing similarity. Error bars
 751 define standard errors.

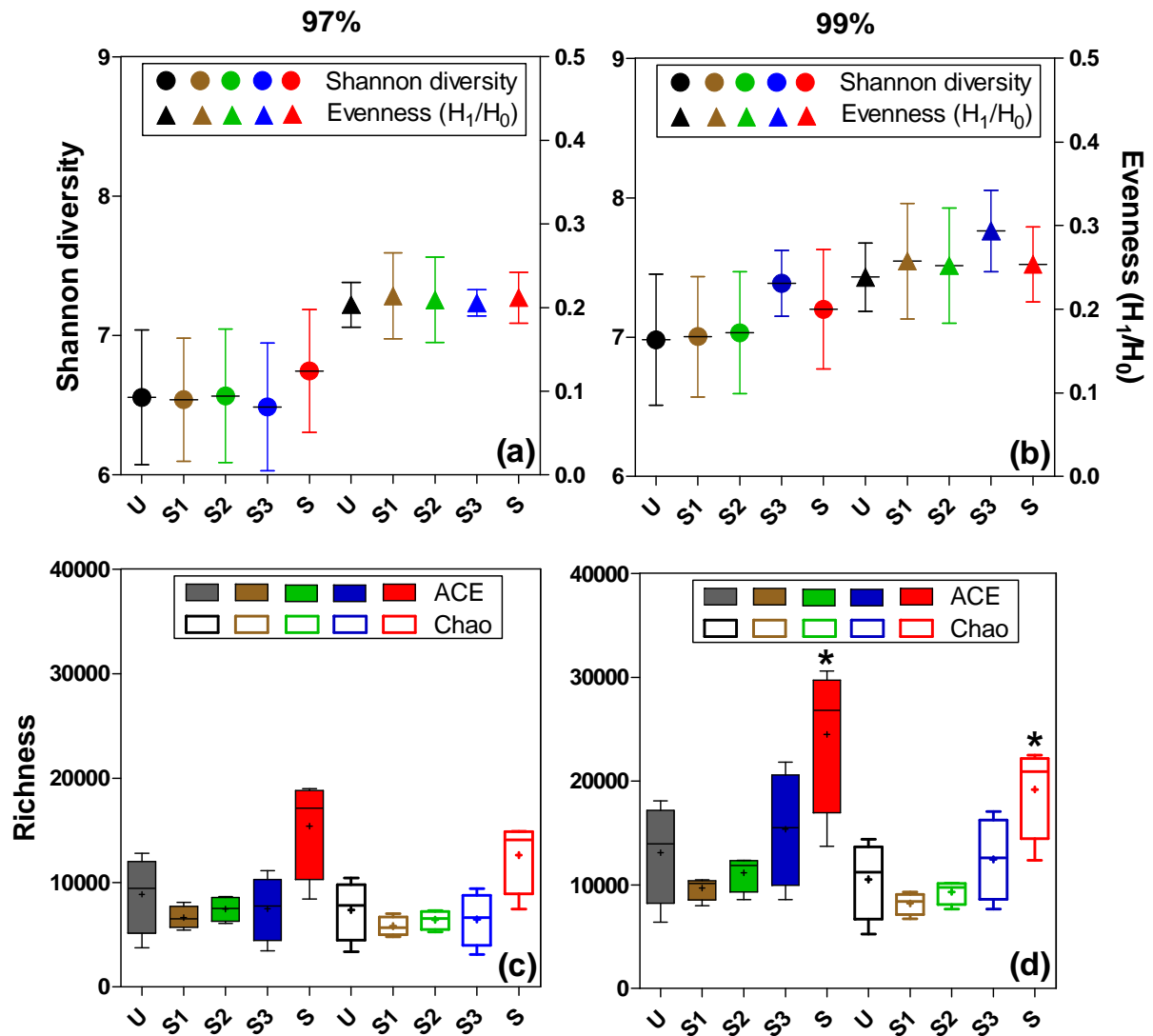
752



753

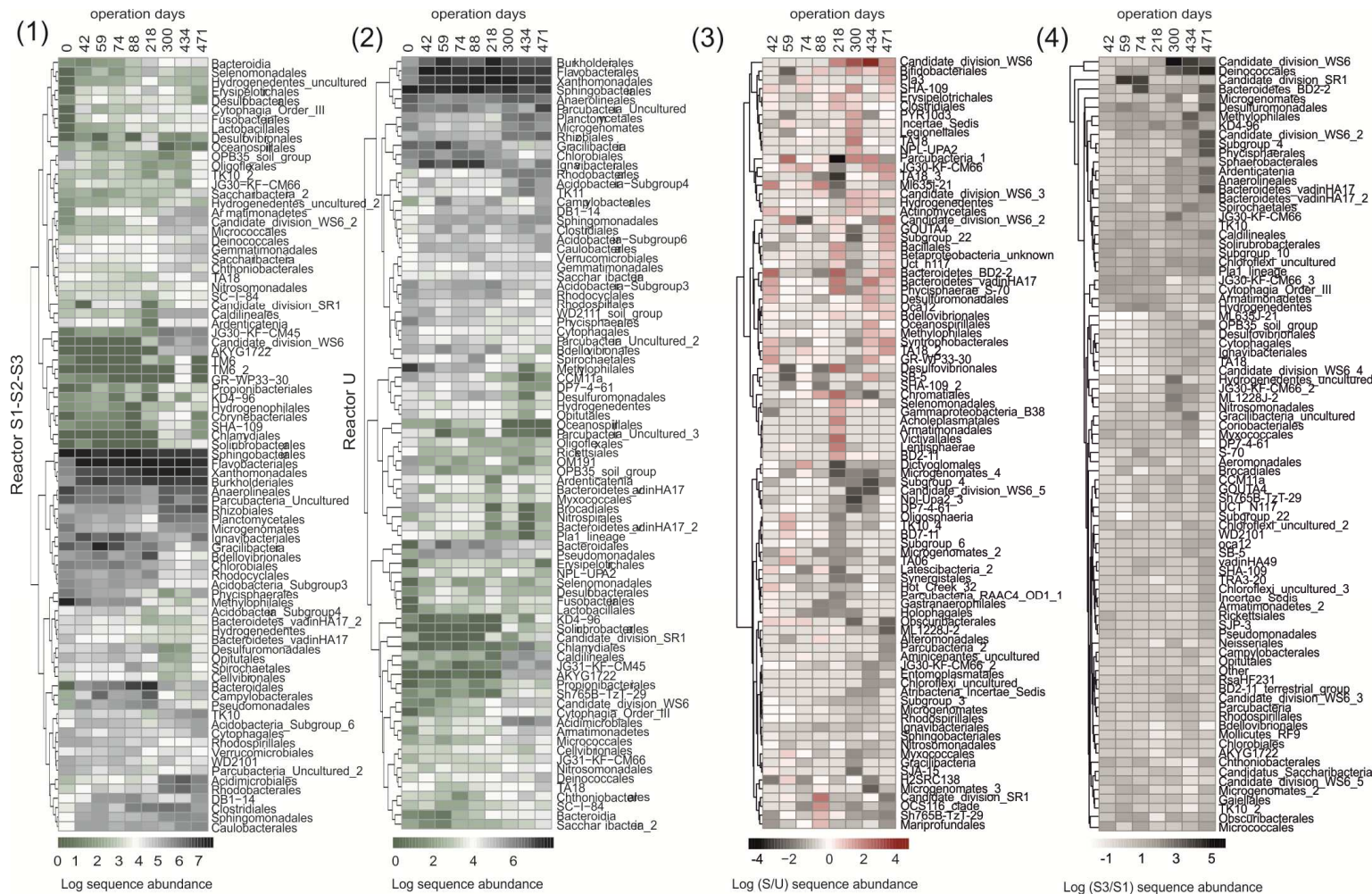
754 **Figure 3.** Moving window analysis (MWA) using reciprocal of Bray-Curtis indices (β) from the initial biofilm
755 inoculum measured at different sequence similarity (93-99%) for S and U over 471 days of operation.

756



757

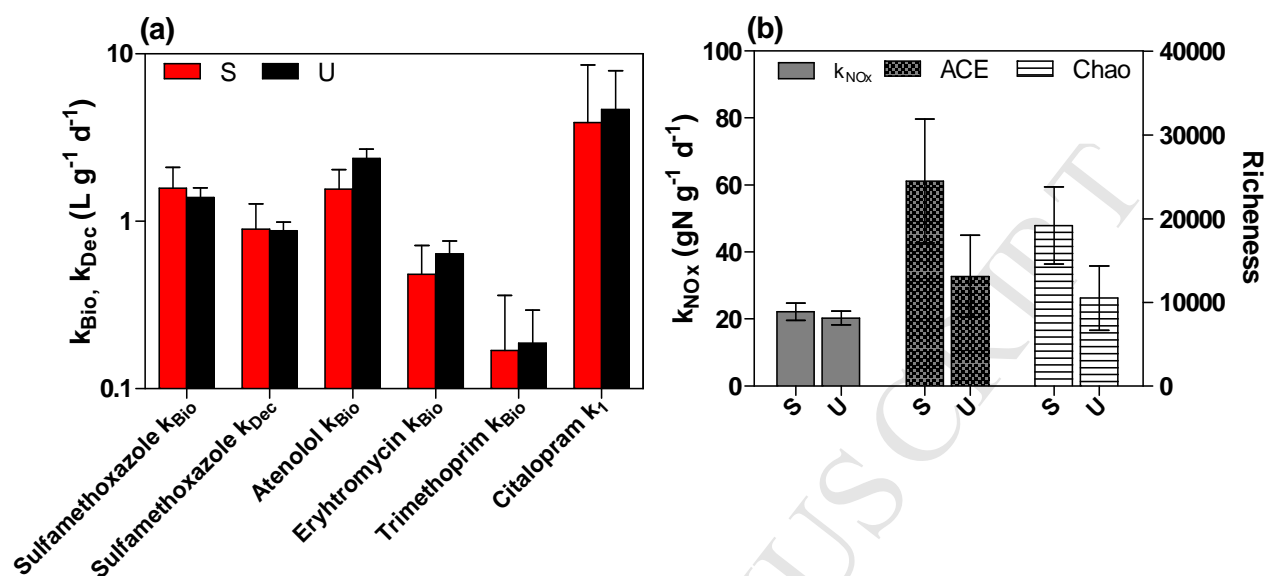
758 **Figure 4.** Averaged values of Shannon diversity, evenness, ACE and Chao indices after 200 days of operation
 759 (n=4) at 97% (a, c) and 99% (b, d) sequence similarity cut-offs for the three stages MBBR at local (S1, S2, S3)
 760 and system (S) level and the single stage system (U). Asterisks indicate significance difference (ANOVA,
 761 $p < 0.05$). Mean is shown as +.



762

763 **Figure 5.** Heatmaps of the 100 most abundant order level taxa in the staged MBBR, S (a) and un-staged MBBR, U (b). The most shifted
 764 abundant taxa (expressed as log sequence abundance) of S and S3 were selected to perform the ratio of S/U (c) and S1/S3 (d) to effectively
 765 identify the selected taxa in S compared to U, and S3 compared to S1

766



767
768

769 **Figure 6.** Biotransformation and retransformation rate constants k_{Bio} and k_{Dec} ($L g^{-1} d^{-1}$) for each micropollutant
770 (a) and specific denitrification rate (k_{NOx}), ACE and Chao indices (b) calculated at system level for S for U
771 (Polesel et al., 2017) MBBR in Batch 2. Abbreviations: k_1 , biotransformation rate constant of enantiomer 1.

772

773

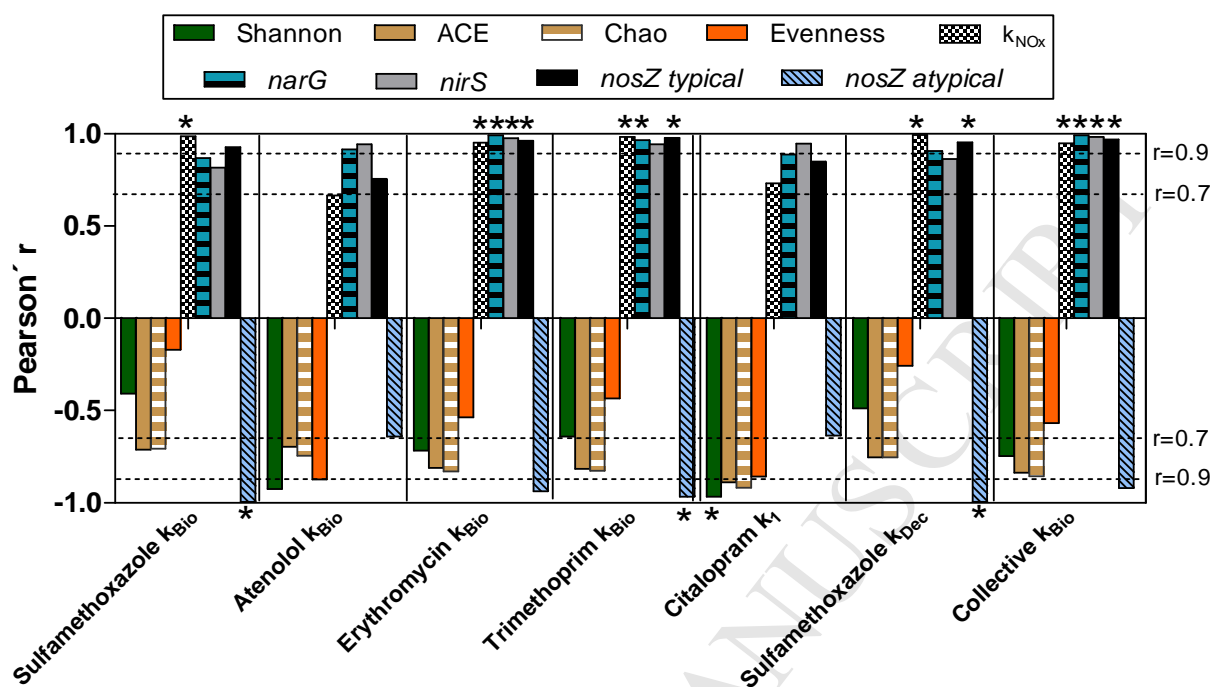
774
775

Figure 7. Pearson's coefficient (r) of the correlation between biotransformation (k_{Bio}), retransformation (k_{Dec}) of micropollutant, collective k_{Bio} with Shannon biodiversity, richness (ACE and Chao), evenness indices (at 99% sequences similarity) and specific denitrification rate k_{NOx} ($mgN\ g^{-1}\ d^{-1}$) for Batch 2. Asterisks indicate significance (ANOVA, $p < 0.05$).

779

780

Highlights

- Microbial composition and diversity in single- and three stage MBBR investigated
- Reactor staging increased overall microbial richness and evenness in staged MBBR
- Microbial diversity increased with decreasing carbon loading in staged MBBR
- Biotransformation of pharmaceuticals positively correlated with denitrifying genes abundance
- Biotransformation of pharmaceuticals did not correlate with microbial diversity